Journal of Applied Physics

RESEARCH ARTICLE | JANUARY 22 2024

A new analytical method for modeling a 2D electrostatic potential in MOS devices, applicable to compact modeling

F. Lime ; B. Iñiguez ; A. Kloes

J. Appl. Phys. 135, 044501 (2024)
https://doi.org/10.1063/5.0188863

AIP Publishing

Journal of Applied Physics METHOD pubs.aip.org/aip/jap

A new analytical method for modeling a 2D electrostatic potential in MOS devices, applicable to compact modeling

Cite as: J. Appl. Phys. **135**, 044501 (2024); doi: 10.1063/5.0188863
Submitted: 24 November 2023 · Accepted: 22 December 2023 ·
Published Online: 22 January 2024

F. Lime,[1,a)] B. Iñiguez,[1] and A. Kloes[2]

AFFILIATIONS

[1]Electronics Engineering Department, Universitat Rovira i Virgili (URV), Tarragona 43007, Spain
[2]Technische Hochschule Mittelhessen, Competence Center for Nanotechnology and Photonics, Wiesenstrasse 14, Giessen 35390, Germany

[a)]**Author to whom correspondence should be addressed:** francois.lime@urv.cat

ABSTRACT

This paper presents a new conformal mapping method to solve 2D Laplace and Poisson equations in MOS devices. More specifically, it consists of an analytical solution of the 2D Laplace equation in a rectangular domain with Dirichlet boundary conditions, with arbitrary values on the boundaries. The advantages of the new method are that all four edges of the rectangle are taken into account and the solution consists of closed-form analytical expressions, which make it fast and suitable for compact modeling. The new model was validated against other similar methods. It was found that the new model is much faster, easier to implement, and avoids many numerical issues, especially near the boundaries, at the cost of a very small loss in accuracy.

I. INTRODUCTION

In semiconductor technologies, compact models are the necessary core component of design tools and circuit simulators. They are needed to reproduce the behavior of the electronic components. These models need to be simple, fast, and efficient in order to allow complex circuit simulations. Over the years, semiconductor devices have been scaled down in order to improve their performance and price per unit. With this size reduction comes new effects to be taken in account, and new architectures have been introduced as well. As a consequence, it becomes more critical to model the device in two or even three dimensions, in addition to the common and usual 1D approach.

For field effect transistors, 2D modeling of the surface potential is necessary in order to take into account short channel effects such as Drain Induced Barrier Lowering (DIBL) and channel length modulation, or even narrow and corner effects in long 3D structures.[1] The various 2D models for compact modeling include the use of an equivalent characteristic length.[2–6] This method has been widely used because of its simplicity, especially when it is not possible to obtain an exact solution. However, this technique is not very accurate for complex and asymmetrical structures. As a more accurate alternative, one can use Fourier series,[7,8] but with the disadvantage of using complex expressions and infinite series. Another possibility is using the conformal mapping technique. The latter is equivalent to Fourier series, but in some cases, it has the advantage of leading to simpler closed-form expressions.[9]

For a MOSFET, conformal mapping was first implemented in Ref. 10 The method has also been used to evaluate fringing fields in SOI technologies.[11,12] The Poisson equation is usually decomposed into the sum of a 1D and a 2D component. The 1D term is a Poisson equation, while the 2D one reduces to the Laplace equation. This is an approximation to simplify the problem. Then, the Laplace equation is solved over a rectangular domain. This is referred to as the 4-corner problem. This has been done for a Double gate MOSFET in Ref. 13. However, the solution of the 4-corner problem is not analytical and, moreover, is computationally expensive. Because of this, the following approximation is usually made. When the rectangle is very long, one of its edges can be neglected as it tends to infinity. This approximation is called the 2-corner problem.[9,14] This method is

usually preferred over the 4-corner one because its solution consists of simple analytical expressions, which are convenient for compact modeling. However, the 2-corner solution becomes inaccurate when the length of the rectangle is less than two times its height.

In this paper, we propose a new approach to the 4-corner problem, which allowed us to obtain a solution that is analytical and uses closed-form expressions, which are desirable in compact models. First, we will explain how to obtain the solution of the Laplace equation on a rectangular domain with the 2-corner method as it is necessary to understand our new method. In the second part, we will explain how to take into account the fourth boundary condition. In the last part, the accuracy of the new 4-corner model will be discussed.

II. LAPLACE AND POISSON EQUATIONS

In semiconductor devices, the electrostatic potential φ and the charges are governed by the Poisson equation. The 2D Poisson equation can be written as

$$\frac{\partial^2\varphi}{\partial x^2}+\frac{\partial^2\varphi}{\partial y^2}=-\frac{\rho}{\varepsilon_{sc}}, \tag{1}$$

where ρ is the charge density and ε_{sc} is the semiconductor permittivity.

Usually, a long channel transistor is governed by the 1D Poisson equation and 2D effects are to be considered only when the channel length is too short. In these cases, 2D effects can be considered as a kind of perturbation to the 1D solution, and the Poisson equation can then be decomposed into a 1D Poisson equation and a 2D Laplace equation,

$$\frac{\partial^2\varphi_{1D}}{\partial x^2}=-\frac{\rho}{\varepsilon_{sc}}, \tag{2}$$

$$\frac{\partial^2\varphi_{2D}}{\partial x^2}+\frac{\partial^2\varphi_{2D}}{\partial y^2}=0, \tag{3}$$

with $\varphi=\varphi_{1D}+\varphi_{2D}$.

With this simplification, we only have to solve Laplace equation (3) in order to obtain the 2D contribution to the potential φ_{2D}. In addition, modern devices usually use low semiconductor doping, and as 2D effects are evaluated below the threshold, it can be considered that $\rho\simeq 0$, so that Poisson equation (1) reduces to Laplace equation (3). For the sake of simplicity, we consider that this is the case in this paper, and we have $\varphi=\varphi_{2D}=V$ and $\rho=0$.

III. THE 2-CORNER PROBLEM

The solution can of the Laplace equation be found using a Schwarz–Christoffel conformal mapping. In this case, the method is analytical and consists of the following equation, which allows to map a rectangle of length L and height H of the (x, y)-plane, as shown Fig. 1, to the upper part of the (u, v)-plane,[14]

$$\mathrm{w}=\mathrm{u}+\mathrm{iv}=\cosh\left(\pi\frac{z}{H}\right), \tag{4}$$

with $z=x+\mathrm{i}y$.

This is equivalent to the following transition equations between x, y and u, v:

$$\mathrm{u}(x,y)=\cosh\left(\pi\frac{x}{H}\right)\cos\left(\pi\frac{y}{H}\right) \tag{5}$$

and

$$\mathrm{v}(x,y)=\sinh\left(\pi\frac{x}{H}\right)\sin\left(\pi\frac{y}{H}\right). \tag{6}$$

The mapping of the rectangle of Fig. 1(a) using (4) is shown Fig. 1(b). The rectangular domain is mapped to the upper half (u, v)-plane, with the right edge of the rectangle on the positive values of the real axis of the complex (u, v)-plane. The top, bottom,

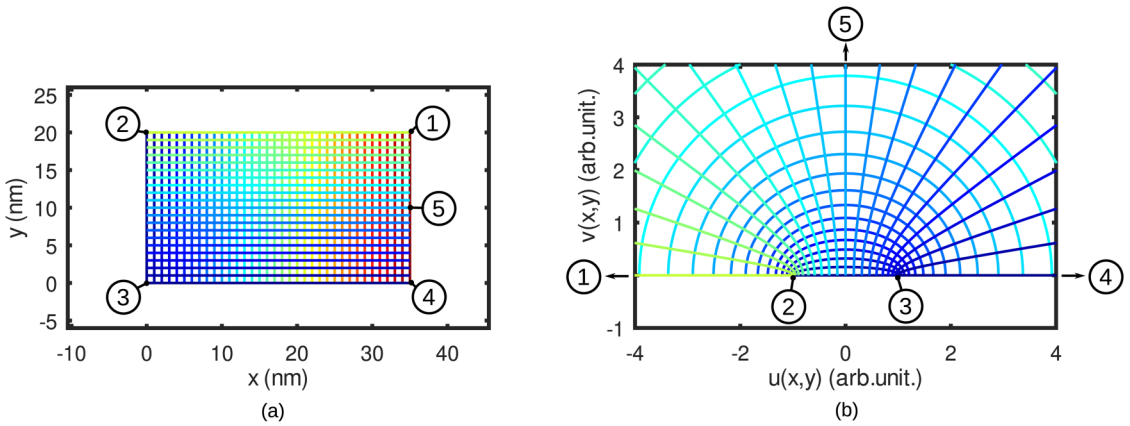

FIG. 1. A rectangular area in the (x, y)-plane of dimensions $L = 35,:\mathrm{nm}$ and $H = 20,:\mathrm{nm}$. The space between the lines is $1,:\mathrm{nm}$ (a). (b) is the same rectangular area being mapped into the (u, v)-plane using (4). The circled numbers show the location of the four corners plus the point of coordinates $(L, H/2)$.

and left edges are mapped to the real axis, while the right edge is mapped to a half ellipse around the point (0,0) whose size increases as L increases. This means that when L tends to infinity, or equivalently $L >> W$, the right edge of the rectangle will effectively be mapped to infinity.

With this assumption that $L >> W$, we can then obtain a solution of the Laplace equation, considering $V = V_0$ on a line located on the boundary of the rectangle of the (x, y)-plane, and $V = 0$ everywhere else on the boundary. It could be, for example, a line between points #2 and #3 in Fig. 1. In the (x, y)-plane, this line is defined between the two points $z_1 = (x_1, y_1)$ and $z_2 = (x_2, y_2)$. In the (u, v)-plane, the line will be located on the real axis between the points $\mathrm{u}(x_1, y_1)$ and $\mathrm{u}(x_2, y_2)$. The solution is then,[10,14,15]

$$\mathrm{V}(x, y) = \frac{V_0}{\pi}\left(f(x, y, x_1, y_1) - f(x, y, x_2, y_2)\right) \tag{7}$$

with

$$f(x, y, x', y') = \arctan\left(\frac{\mathrm{u}(x, y) - \mathrm{u}(x', y')}{\mathrm{v}(x, y)}\right) \tag{8}$$

and where u and v are, respectively, given by (5) and (6). This is the solution of the 2-corner problem, that is to say, when the right-hand side boundary condition is not applied. It is strictly valid if the line is located far away from the opposite side of the rectangle so that the potential at the missing boundary is close to 0. In order to take into account the third edge of the rectangle, i.e., the right-hand side boundary condition in our example, we need to solve the 4-corner problem. This is required when $H \simeq L$.

IV. A NEW APPROACH FOR THE 4-CORNER PROBLEM

The solution of the 4-corner problem is already known and can be found in some textbooks on complex analysis.[15] It is also based on a Schwarz–Christoffel conformal mapping. This method has been implemented for a Double Gate MOSFET in Ref. 13. However, this solution requires finding an inverse function for elliptic integrals. Thus, it is a numerical method and is not analytical. In the following, we propose a new approach that is not based on the Schwarz–Christoffel conformal mapping. This new model does not require the evaluation of elliptic integrals and has the advantage of being analytic. However, we will also show that the new method is only a good approximation to the exact Schwarz–Christoffel approach.

The method consists of applying a map, which converts the 4-corner problem into a 2-corner one. Such a map is the following one:

$$Z_1 = \mathrm{X}_1 + \mathrm{i}\mathrm{Y}_1 = \ln\left(\frac{\cosh\left(\pi\frac{L}{H}\right)}{\cosh\left(\pi\frac{L-z}{H}\right)}\right). \tag{9}$$

First, it should be shown that the map (9) is conformal, i.e., that Laplace equation is invariant to this mapping. This can be done using the property that any combination of two conformal maps is also conformal. In fact, $\cosh(z)$ is conformal as well as $\ln(z)$, except when $|z| = 0$. This means that (9) is conformal, except at the point #5 in Fig. 1, which is the point of coordinates $(L, H/2)$. As this point is situated on the boundary of the domain, where the potential is known, the method will not be applied at this particular point and this should not be an issue.

The result of applying (9) to the domain of Fig. 1 is shown Fig. 2. Basically, the geometry is unaffected except for the right-hand side boundary of the rectangle that is opened up toward infinity. In other words, Eq. (9) maps the upper part of the right-hand side of the rectangle (i.e., the boundary points situated between the circled numbers #1 and #5 in Fig. 1(a)) to the upper side and the lower part (the points between circled numbers #4 and #5) to the bottom edge. The middle point $(L, H/2)$, labeled as circled number #5 in the figure, is mapped to infinity. The vertical left-hand side of the rectangle is mapped between 0 and π but is not completely straight anymore. With that reserve in mind, which will have consequences explained latter, we can say that we just approximately converted the 4-corner problem to a 2-corner one, whose solution can be found with Eqs. (4–8). More specifically, we combine (9) with (4) in order to align the four edges to the real axis of the w-plane. This gives the following map:

$$\mathrm{w} = \cosh(Z_1(x, y)) \tag{10}$$

or, equivalently,

$$\mathrm{w} = \mathrm{u} + \mathrm{iv} = \frac{1}{2}\left(\frac{\cosh\left(\pi\frac{L}{H}\right)}{\cosh\left(\pi\frac{L-z}{H}\right)} + \frac{\cosh\left(\pi\frac{L-z}{H}\right)}{\cosh\left(\pi\frac{L}{H}\right)}\right), \tag{11}$$

with

$$\mathrm{u}(x, y) = \frac{\cosh\left(\pi\frac{L-x}{H}\right)\cos\left(\pi\frac{y}{H}\right)}{2\cosh\left(\pi\frac{L}{H}\right)}\left(\frac{\cosh^2\left(\pi\frac{L}{H}\right)}{\sinh^2\left(\pi\frac{L-x}{H}\right) + \cos^2\left(\pi\frac{y}{H}\right)} + 1\right), \tag{12}$$

$$\mathrm{v}(x, y) = \frac{\sinh\left(\pi\frac{L-x}{H}\right)\sin\left(\pi\frac{y}{H}\right)}{2\cosh\left(\pi\frac{L}{H}\right)}\left(\frac{\cosh^2\left(\pi\frac{L}{H}\right)}{\sinh^2\left(\pi\frac{L-x}{H}\right) + \cos^2\left(\pi\frac{y}{H}\right)} - 1\right). \tag{13}$$

The result of the map (11) is shown Fig. 3 for the case $H = L$. The four corners, labeled with circled numbers 1–4 in Figs. 1 and 3, are mapped to the real axis: two at ± 1 and the other two

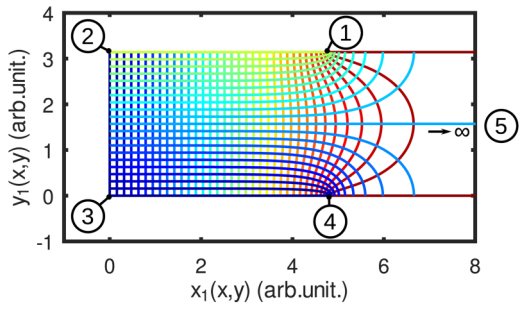

FIG. 2. The rectangular area of Fig. 1(a) after being mapped into the $(\mathrm{X}_1, \mathrm{Y}_1)$-plane using (9).

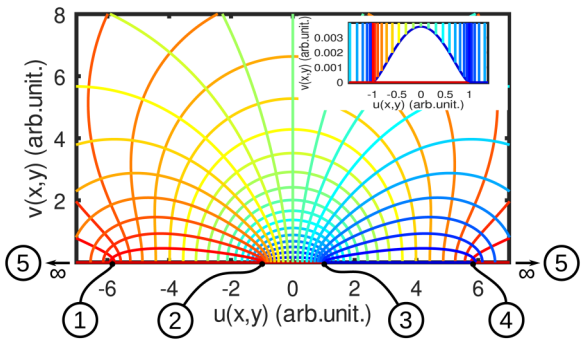

FIG. 3. The rectangular area of Fig. 1 after being mapped into the w-plane using (11), for the case $H = L$. The left-hand edge of the rectangle is mapped to the values of the real axis u between −1 and 1. Inset: a close-up showing the deviation from the real axis when $-1 < u < 1$. The maximum deviation is at most 0.0038 at u = 0. The four corners and the point $(L, H/2)$ are indicated with a circled number.

at $\pm 5.84 = (\cosh(\pi) + 1/\cosh(\pi))/2$, obtained from (11) when $z = L = H$. The boundary is mapped to the real axis as follows. The left-hand side is mapped to the values $-1 < u < 1$, the top side to $-5.84 < u < -1$, and the bottom edge to $1 < u < 5.84$. As for the upper half of the right side, it is mapped to the interval $-\infty < u < -5.84$, while the lower half corresponds to $5.84 < u < \infty$.

However, (11) is only an approximation for the 4-corner problem, as the left-hand edge is not exactly mapped to the real axis, but very close to it, as shown by the inset of Fig. 3. As a consequence, the value obtained when solving the Laplace equation at the left-hand side will be a little underestimated. The reason for this error is due to the map (9). This can be seen in Fig. 2 as the vertical lines, which are close to the right-hand side are not straight anymore but deformed in the center. This effect becomes weaker the closer we are to the left-hand side of the rectangle but never disappears completely. This means that the approximation is better for higher L/H ratios. However, the accuracy is still acceptable for the limiting case $L = H$, with a deformation of less than 1% at the left-hand side. From the inset of Fig. 3, it can be seen that the left-hand side of the rectangle is approximately mapped to the real axis between $u = -1$ and $u = 1$, with a value of 0.0037 for the maximum deviation from the real axis at $u = 0$. This represents 0.185% of the length of this side of the rectangle in the (u,v)-plane, which is equal to 2. As this deformation is quite small, we consider the map (11) to be a good approximation for the 4-corner problem, provided that $L > H$.

For the cases when $L < H$, the problem should be rotated 90°. This can be done easily in equations (12) and (13) by inverting x and y, L, and H and also changing the sign of u. This gives

$$u(x,y) = -\frac{\cosh\left(\pi\frac{H-y}{L}\right)\cos\left(\pi\frac{x}{L}\right)}{2\cosh\left(\pi\frac{H}{L}\right)}\left(\frac{\cosh^2\left(\pi\frac{H}{L}\right)}{\sinh^2\left(\pi\frac{H-y}{L}\right)+\cos^2\left(\pi\frac{x}{L}\right)}+1\right), \tag{14}$$

$$v(x,y) = \frac{\sinh\left(\pi\frac{H-y}{L}\right)\sin\left(\pi\frac{x}{L}\right)}{2\cosh\left(\pi\frac{H}{L}\right)}\left(\frac{\cosh^2\left(\pi\frac{H}{L}\right)}{\sinh^2\left(\pi\frac{H-y}{L}\right)+\cos^2\left(\pi\frac{x}{L}\right)}-1\right). \tag{15}$$

The solution of the potential using the Laplace equation can obtained with (7) for a constant value on the boundary between the points z_1 and z_2, considering z_2 to be after z_1 in an anticlockwise way around the boundary. However, when the point $(L, H/2)$ is between z_1 and z_2, (7) have to be replaced by

$$V(x,y) = V_0 + \frac{V_0}{\pi}\left(f(x,y,x_1,y_1) - f(x,y,x_2,y_2)\right) \tag{16}$$

because the line is going from $+\infty$ to $-\infty$ in the (u, v)-plane. This can be useful as the error explained above is mainly located on the left-hand side of the domain, so in some cases, it might be more interesting to apply the boundary condition to the right-hand side.

When V_0 is a function of y, we can use the superposition principle to obtain an approximated solution, as shown in this example for the left-hand side of the rectangular domain,

$$V(x,y) = \sum_{n=1}^{N-1}\frac{V_0(y_n) + V_0(y_{n+1})}{2\pi}\left(f(x,y,0,y_{n+1}) - f(x,y,0,y_n)\right), \tag{17}$$

with

$$y_n = y_1 + \frac{y_2 - y_1}{N}n.$$

The desired number of intermediary values of $V_0(y)$ between y_1 and y_2 is $N - 1$.

Using (17), it is then possible to obtain an approximated analytical and explicit expression for the solution of the Laplace equation, with arbitrary Dirichlet boundary conditions on the rectangular domain.

To illustrate the accuracy of the new method, we show the following example. A domain with $H = L = 12$ nm is considered with the potential equal to 1 V on the left-hand side of the rectangle and 0 everywhere else on the boundary. The results for the 4- and 2-corner cases are plotted against x in Fig. 4, for $y = H/2$. It can be observed that, for the 4-corner case, the potential correctly cancels to 0 on the right-hand side, in contrast to the 2-corner one, because the fourth boundary condition is not applied in that case. The 4-corner approach is much more accurate than the 2-corner one, especially when L becomes comparable to H and the 2-corner method fails. This figure also compares the new model with the original Schwarz–Christoffel numerical 4-corner model.[13] The agreement with our 4-corner model is excellent. This shows that the approximations of the analytical model have a very low impact on the results, even for the worst case $H = L$. In addition, our model is much faster and, being analytical, does not suffer from the numerical inaccuracies inherent to the

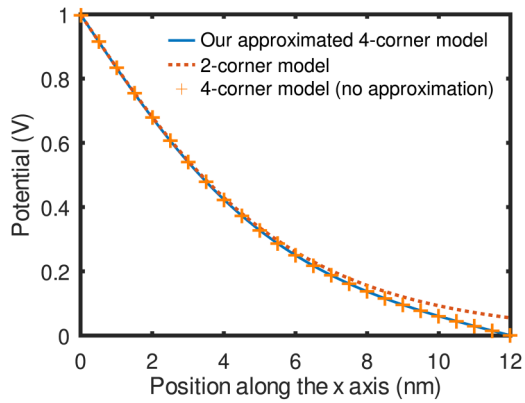

FIG. 4. The potential at $y = H/2$, for the following boundary conditions: $V = 1V$ on the left-hand side and 0 everywhere else, for the case $H = L$. The 4- and 2-corner cases are compared. Symbols are the 4-corner model without approximation, presented in Ref.[13].

4-corner Schwarz–Christoffel method. These inaccuracies of the Schwarz–Christoffel model come from the use of complex integrals and interpolations, generally over quantities, which tend to infinity.

V. A SIMPLE EXAMPLE FOR A DOUBLE GATE MOSFET

As explained below (16), we can assign non zero values to the boundary condition on the right-hand edge of the domain, or to the left-hand one, which is easier to implement. We give the following example for the right-hand case. We first calculate the potential for the right-hand side of the channel, i.e., for $x > L/2$. The contribution from the drain was obtained from (16) as follows. As the boundary condition line is crossing the point $(L, H/2)$, we have to use (16) instead of (7),

$$V_{drain}(x, y) = V_D + \frac{V_D}{\pi}\left[f(x, y, L, t_{oxb}) - f\left(x, y, L, H - t_{oxf}\right)\right]. \quad (18)$$

Where t_{oxf} and t_{oxb} are, respectively, the equivalent thicknesses of the front and back gate dielectrics. In a similar way, contributions from the top and back gate were obtained from (7),

$$V_{topgate}(x, y) = \frac{V_{Gt}}{\pi}\left(f(x, y, L, H) - f(x, y, 0, H)\right), \quad (19)$$

$$V_{backgate}(x, y) = \frac{V_{Gb}}{\pi}\left(f(x, y, 0, 0) - f(x, y, L, 0)\right). \quad (20)$$

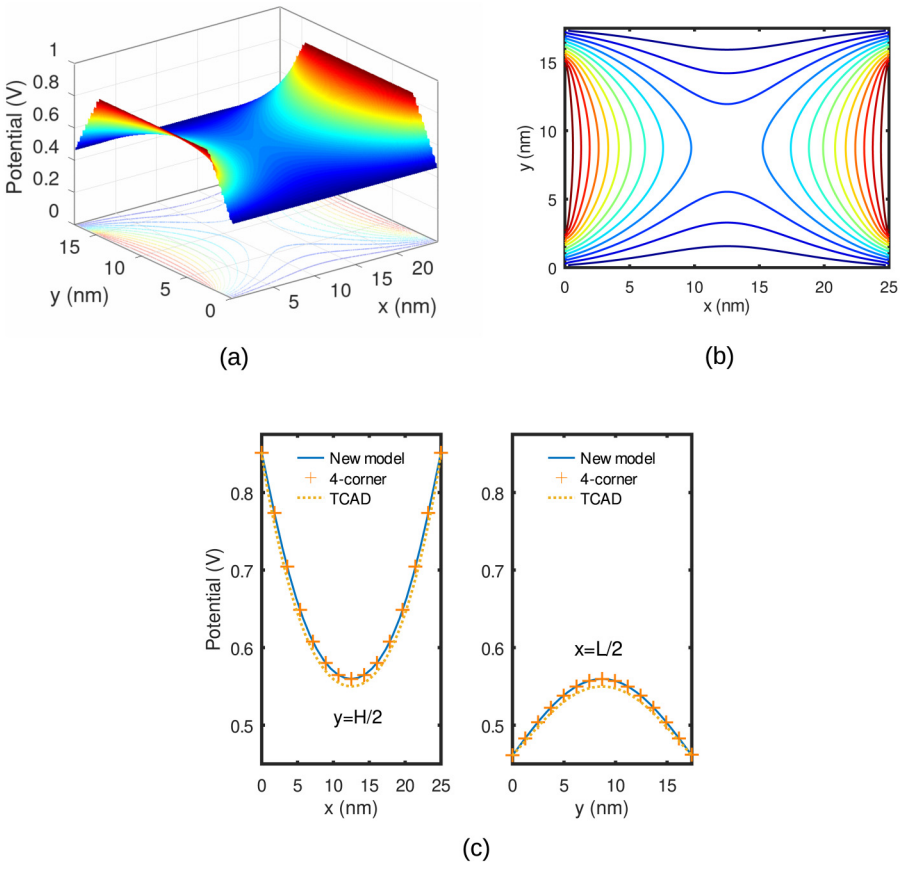

FIG. 5. (a) The calculated 2D potential from our model, for a Double Gate MOSFET with $t_{sc} = 12$ nm, $t_{ox} = 1.6$ nm, and $L = 25$ nm. (b) Corresponding equipotentials. (c) Horizontal and vertical cuts of the potential shown in (a), at the center of the channel. Lines are our model, dotted lines are from TCAD Silvaco, and symbols are the 4-corner Schwarz–Christoffel model from Kolberg *et al.*[13]

The contribution from the top and back gate dielectrics V_{oxt} and V_{oxb} were obtained from (17). Considering, as an approximation, a linear potential drop in the dielectrics, the following Dirichlet boundary condition were considered in the front and back gate insulators: $V_{0xt}(y) = V_{Gt} + (V_S - V_{Gt})(H - y)/t_{oxf}$ and $V_{0xb}(y) = V_{Gb} + (V_S - V_{Gb})y/t_{oxb}$. In this case, we also used equivalent oxide thicknesses in order to avoid discontinuity in the permittivity.

Summing all the contributions gives the contribution for the right-hand side of the channel

$$V_R(x, y, V_D) = V_{drain}(x, y, V_D) + V_{oxt}(x, y, V_D) + V_{oxb}(x, y, V_D). \quad (21)$$

The contribution from the left side was obtained "mirroring" V_R with respect to the middle of the channel, so that the total potential, including the contributions from the top and back gates, is

$$V_{tot}(x, y) = V_R(x, y, V_D) + V_R(L - x, y, V_S) + V_{topgate}(x, y) + V_{backgate}(x, y). \quad (22)$$

To validate our model, we compared it with a similar method published in Ref. 13, which used a Schwarz–Christoffel conformal mapping, that is to say, the original 4-corner method, without approximation, which is not analytical. We implemented their method and reproduced the example given in their paper, which consists of DGMOS with 25 nm for the gate length, a silicon thickness of 12 nm, a gate oxide thickness of 1.6 nm, and an aluminum gate. The results are shown in Fig. 5. We used equivalent gate dielectric thicknesses $t_{ox}^{eq} = t_{ox}\varepsilon_{sc}/\varepsilon_{ox}$ in order to avoid the discontinuity in the two relative permittivity values, which are $\varepsilon_{sc} = 11.8$ for the semiconductor and $\varepsilon_{ox} = 7$ for the dielectrics. As an improvement over,[13] a linear boundary condition in the gate dielectric was also considered with 10 intermediary values, i.e., N = 10 in (17). Figure 5(a) shows the 2D potential obtained from our model, i.e., Equation (22), and (b) shows the corresponding equipotentials. In this former figure, the source is located on the left, the drain on the right, the top gate on the top and the back gate on the bottom of the rectangle. The linear potential in the dielectrics, along with the ten intermediary steps can also be seen in Fig. 5(a). In Fig. 5(c), our model is compared with both the Schwartz–Cristoffel 4-corner method of Ref. 13 and with Technology Computer-Aided Design (TCAD) simulations done with Silvaco Atlas. Figure 5(c) shows two cuts of the 2D potential of (a): a vertical one at $x = L/2$ and a horizontal one at $y = H/2$. The comparison between the two 4-corner approaches shows very similar results, which validates our method. The two characteristics are nearly identical, but our analytical model should give a better representation of the 2D potential in the gate dielectrics, especially near the boundary conditions and the corners, because in those areas it is difficult to evaluate the numerical approach with a high enough precision. The small discrepancy with TCAD could be due to the source/drain junction built-in potential, that is to say, the boundary value at the source and drain end of the channel, as we could achieve a much better fit with the lower value of this built-in potential. This may be explained as in reality, this potential is not applied exactly at the boundary of the channel but more inside the source and drain regions.[16]

VI. CONCLUSIONS

In this work, a new technique to model a 2D potential in MOS devices has been presented. It is based on a conformal mapping method to solve the Laplace equation on a rectangular domain. The new model takes into account all four edges of the rectangle, and only needs the values on the boundary to be defined. The solution presents the advantage of being constituted of closed-form analytical expressions. These are similar in complexity to the solution of the 2-corner problem. The accuracy was found to be excellent and the new technique was found to be a very good approximation of the 4-corner method. Compared to the 4-corner method, the new model is much faster, easier to implement, and avoid many numerical issues, especially near the boundaries. The trade-off is a small, negligible loss in accuracy. Thanks to these characteristics, the new model is suitable for compact modeling and should be especially useful when modeling very short-channel FETs.

ACKNOWLEDGMENTS

This work was funded by the Spanish Ministry of Science through Contract No. PRX21/00726.

AUTHOR DECLARATIONS

Conflict of Interest

The authors have no conflicts to disclose.

Author Contributions

F. Lime: Conceptualization (lead); Investigation (lead); Methodology (lead); Validation (lead); Writing – original draft (lead). **B. Iñiguez:** Investigation (equal); Supervision (equal); Writing – review & editing (equal). **A. Kloes:** Investigation (equal); Supervision (equal); Writing – review & editing (equal).

DATA AVAILABILITY

Data sharing is not applicable to this article as no new data were created or analyzed in this study.

REFERENCES

[1]A. Kloes, M. Weidemann, D. Goebel, and B. T. Bosworth, "Three-dimensional closed-form model for potential barrier in undoped FinFETs resulting in analytical equations for V_T and subthreshold slope," IEEE Trans. Electron Devices **55**, 3467–3475 (2008).

[2]R.-H. Yan, A. Ourmazd, and K. F. Lee, "Scaling the Si MOSFET: From bulk to SOI to bulk," IEEE Trans. Electron Devices **39**, 1704–1710 (1992).

[3]K. Suzuki, T. Tanaka, Y. Tosaka, H. Horie, and Y. Arimoto, "Scaling theory for double-gate SOI MOSFET's," IEEE Trans. Electron Devices **40**, 2326–2329 (1993).

[4]F. Lime, B. Iniguez, and O. Moldovan, "A quasi-two-dimensional compact drain–current model for undoped symmetric double-gate MOSFETs including short-channel effects," IEEE Trans. Electron Devices **55**, 1441–1448 (2008).

[5]A. Yesayan, F. Prégaldiny, N. Chevillon, C. Lallement, and J.-M. Sallese, "Physics-based compact model for ultra-scaled FinFETs," Solid-State Electron. **62**, 165–173 (2011).
[6]A. Dey, A. Chakravorty, N. DasGupta, and A. DasGupta, "Analytical model of subthreshold current and slope for asymmetric 4-T and 3-T double-gate MOSFETs," IEEE Trans. Electron Devices **55**, 3442–3449 (2008).
[7]X. Liang and Y. Taur, "A 2-D analytical solution for SCEs in DG MOSFETs," IEEE Trans. Electron Devices **51**, 1385–1391 (2004).
[8]R. Ritzenthaler, F. Lime, O. Faynot, S. Cristoloveanu, and B. Iñiguez, "3D analytical modelling of subthreshold characteristics in vertical Multiple-gate FinFET transistors," Solid-State. Electron. **65–66**, 94–102 (2011).
[9]M. Schwarz, M. Weidemann, A. Kloes, and B. Iñíguez, "2D analytical calculation of the electrostatic potential in lightly doped Schottky barrier double-gate MOSFET," Solid-State. Electron. **54**, 1372–1380 (2010).
[10]A. Kloes and A. Kostka, "A new analytical method of solving 2D Poisson's equation in MOS devices applied to threshold voltage and subthreshold modeling," Solid-State. Electron. **39**, 1761–1775 (1996).
[11]T. Ernst, C. Tinella, C. Raynaud, and S. Cristoloveanu, "Fringing fields in sub-0.1 μm fully depleted SOI MOSFETs: Optimization of the device architecture," Solid-State. Electron. **46**, 373–378 (2002).
[12]T. Ernst, R. Ritzenthaler, O. Faynot, and S. Cristoloveanu, "A model of fringing fields in short-channel planar and triple-gate SOI MOSFETs," IEEE Trans. Electron Devices **54**, 1366–1375 (2007).
[13]S. Kolberg and T. A. Fjeldly, "2D modelling of nanoscale double gate silicon-on-insulator MOSFETs using conformal mapping," Phys. Scr. **T126**, 57–60 (2006).
[14]M. Schwarz, T. Holtij, A. Kloes, and B. Iñíguez, "Analytical compact modeling framework for the 2D electrostatics in lightly doped double-gate MOSFETs," Solid-State. Electron. **69**, 72–84 (2012).
[15]E. Weber, *Electromagnetic Fields: Mapping of Fields*, Electromagnetic Fields, Vol. 1 (Wiley, 1950).
[16]T. Dutta, Q. Rafhay, G. Pananakakis, and G. Ghibaudo, "Modeling of the impact of source/drain regions on short channel effects in MOSFETs," in *2013 14th International Conference on Ultimate Integration on Silicon (ULIS)* (IEEE, 2013) pp. 69–72.